Vol. 14, No. 1 (2025): 118 - 129 http://dx.doi.org/10.23960/jtep-l.v14i1.118-129

JURNAL TEKNIK PERTANIAN LAMPUNG

ISSN 2302-559X (print) / 2549-0818 (online)
Journal homepage : https://jurnal.fp.unila.ac.id/index.php/JTP

ORC Performance Study with R32 and R134a Using Biomass as an Energy Source

Lalu Muh Fathul Aziz Al azhari[1], Muhamad Yulianto[1,✉], Edy Hartulistiyoso[1]

[1] Department of Mechanical and Biosystem Engineering, Faculty of Agricultural Engineering and Technology, IPB University, Bogor, INDONESIA

Article History:

Received : 01 July 2024
Revised : 11 August 2024
Accepted : 20 August 2024

Keywords:

LCCP,
Organic rankine cycle,
R134a,
R32,
Simulation,
Work output.

Corresponding Author:
✉ muhamad_yulianto@apps.ipb.ac.id
(Muhamad Yulianto)

ABSTRACT

The use of fossil energy as the main source of primary energy reached 84.7%, with electricity consumption in Indonesia of 1,173 kWh/capita, dominated by fossil fuels (67.21%). The decline in fossil energy reserves requires the development of alternative technologies such as the Organic Rankine Cycle (ORC) that can operate at low to medium temperatures (60°C-200°C). This research was carried out in 2 ways, experiment, and simulation. Experiments were carried out to determine the temperature that can be generated in the evaporator of ORC from the flue gas flow from burning biomass. Simulations were carried out to evaluate the performance of the ORC cycle with working fluids R32 and R134a and the contribution of CO_2 to the environment using the LCCP (Life Cycle Climate Performance) method. The analysis involves measuring the outlet temperature of the evaporator. The research results show that the validation for predicting the output temperature of the ORC evaporator is very good with a Mean Absolute Percentage Error (MAPE) value of <10%. Simulation results show that in this study, R32 performed better than R134a, with a net power of 0.13 kW at a temperature of 86.83°C. LCCP analysis results show that R32 has lower direct emissions than R134a, with better LCCP values.

1. INTRODUCTION

The use of fossil energy to meet primary energy needs such as coal reaches 84.7% (Zhang *et al*., 2021). Electricity consumption in Indonesia reaches 1,173 kWh/capita with fossil fuel power generation sources reaching 67.21%, in contrast to Indonesia's commitment to reduce greenhouse gas (GHG) emissions by 31.89% by 2030 (Kementerian ESDM, 2023). The depletion of these energy source reserves is a challenge for the development of thermal systems that can utilize low-grade heat sources for power generation systems (Ashwni *et al*., 2021).

One alternative technology to overcome this problem is the Organic Rankine Cycle (ORC) which is capable of operating at low to medium temperatures with a range of 60℃-200℃ (Zhao *et al*., 2018). ORC using R134a working fluid at an operating temperature of 60°C has been simulated, the results of the study show that the thermal efficiency of the ORC system reaches 5.60% (Sucahyo *et al*., 2019). ORC is the basic working cycle of the rankine cycle which includes the basic processes of compression, evaporation, expansion and condensation (Macchi & Astolfi, 2017). The main components of ORC are generally the same as the conventional Rankin cycle consisting of a pump, evaporator, expander and condenser. The ORC cycle can be seen in Figure 1. The working fluid heating process in this study uses direct heating from the flue gas heat generated in the biomass combustion process in the combustion furnace, the processes that occur in the system that we observe are as follows:

a. Process 1 to 2 is the compression of the working fluid in the pump
b. Process 2 to 3 is the transfer of heat and mass in the boiler

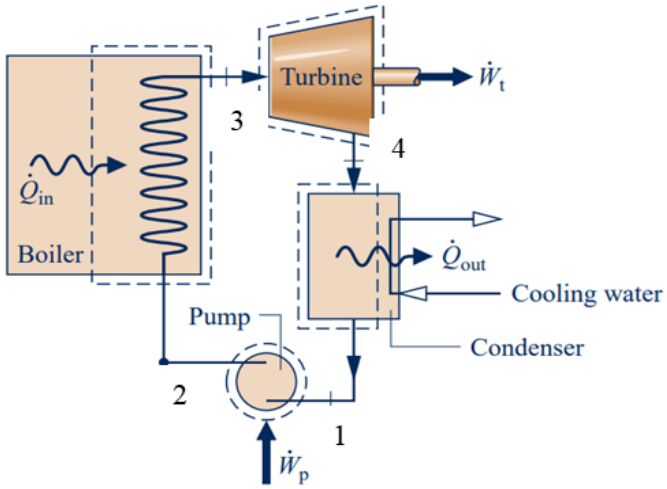

Figure 1. Schematic diagram of ORC cycle

c. Process 3 to 4 is the expansion process in the expander
d. Process 4 to 1 is the process of releasing working fluid heat in the condenser

In general, the working fluids used in the ORC cycle are Chlorofluorocarbons (CFCs), Aromatic Hydrocarbons, Hydrofluorocarbons (HFCs), Hydrocarbons (HCs), Hydrofluoroolefins (HFOs) and Siloxanes (Dai *et al*., 2019). This makes ORC an interesting topic among researchers of thermal systems and renewable energy, and has grown rapidly worldwide in recent years. Muslim *et al*. (2019), observed ORC with temperature parameters on each component, then simulated it on Cycle Tempo software to estimate the output power using R134a working fluid. Thangavel *et al*. (2021), observed the difference in working fluids on ORC performance, the results showed that R134a was better than R290. Other researchers, Hijriawan *et al*. (2022), conducted an experimental study using R134a working fluid with a scroll-expander, the net power generated in the study was 584.5 W. Research report by Bahrami *et al*. (2022), combined Life Cycle Analysis (LCA) and techno-economic analysis to assess ORC performance, the approach provides good environmental performance throughout its life cycle. The use of biomass to generate heat and power is an effective and efficient option for generating heat. Among the renewable biomass energy that has been introduced by researchers to be developed on an industrial scale is wood (Ono *et al*., 2023). Agricultural byproducts such as wood, rice husk, corn waste, and coconut shells are abundant and can be an excellent energy source, particularly for direct combustion in boilers (Yulianto *et al*., 2022). By utilizing unused wood waste or even the use of wood plants that are specifically planted as energy crops, it is possible to use it as a sustainable energy source (Alao *et al*., 2022). There are 3 types of wood that can possibly be developed in Indonesia, namely Kaliandra (*Calliandra calothyrsus*), Gamal (*Gliricidia sepium*), and Sengon (*Paraserianthes falcataria*) (Amirta *et al*., 2016).

Based on the existing problems and potentials, the purpose of this study is to evaluate the ORC cycle using working fluids R32 and R134a. Experiments and simulations were carried out to determine the potential of fluegas that can be used to increase the temperature and pressure in the evaporator, to determine the temperature and pressure at the inlet and outlet of each other ORC component such as turbines, condensers, and pumps. The validation conducted was on the outlet temperature side of the ORC evaporator as the core of the heat needed to evaporate the ORC working fluid. Other parameters calculated and analyzed were the output power and also the emission values produced using the LCCP method.

2. MATERIALS AND METHODS

2.1. Materials

The refrigerants used in this study were R32 and R134a. The properties of both refrigerants were known based on Refprop 10.0 software as seen in Table 1.

Table 1. Properties of R32 and R134a

No	Properties	Flue gas	R32	R134a	Unit
		Value	Value	Value	
1	Density	0.62	1.81	3.35	kg/m^3
2	Fluid conductivity	0.044	0.016	0.0294	$W/m℃$
3	Kinematic viscosity	4×10^{-5}	7×10^{-5}	5×10^{-5}	m^2/s
4	Specific heat	1.0557	0.91	0.96	$kJ/kg℃$
5	Mass flow rate of fluid	0.0156	0.0054	0.0054	kg/s
6	Prandtl Number	0.704	0.824	0.734	
7	Flue gas inlet temperature (T_i)	150	30	30	℃
7	Evaporator length	0.97			m

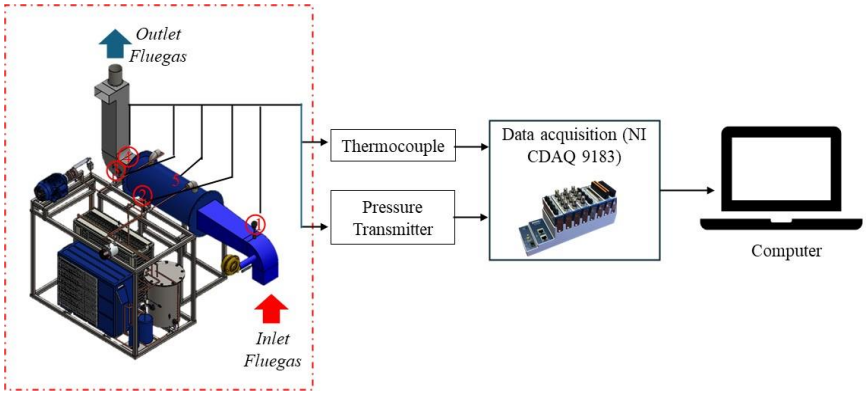

Figure 2. Experimental set-up. (1: Flue gas inlet, 2: R134a and R32 outlet, 3: R134a and R32 inlet, 4: flue gas outlet, 5: Evaporator)

2.2. Research Method

2.2.1. Experimental Set Up

The experimental set-up used in this study can be seen in Figure 2. Temperature measurements at each inlet and outlet of each component use a type K thermocouple. Pressure measurements use a pressure transmitter at the inlet and outlet of each component. Both measurements are connected to data acquisition for data collection. Meanwhile, the mass flow rate of flue gas is measured using a pitot tube.

2.2.2. Simulation Method

The calculation flow in the simulation used is based on the diagram scheme shown in Figure 3. The power generated in the system uses a general relation (Equation 1 and 2) as done by (Hartulistiyoso *et al*., 2020).

$$\boldsymbol{W_{eksp} = m_{ref}(h_{eksp,o} - h_{eksp,i})} \quad (1)$$

$$\boldsymbol{W_p = m_{ref}(h_{p,o} - h_{p,i})} \quad (2)$$

where W_{eksp} is expander power (kW), W_p is pump power (kW), m_{ref} is refrigerant mass rate (kg/s), $h_{eksp,i}$ is inlet enthalpy (kJ/kg), $h_{eksp,o}$ is outlet enthalpy (kJ/kg), $h_{p,i}$ is pump inlet enthalpy (kJ/kg), and $h_{p,o}$ is pump outlet enthalpy (kJ/kg).

Predicting the temperature of the working fluid leaving the evaporator requires calculating the heat transfer coefficient, total heat transfer coefficient and logarithmic average temperature difference. Calculation of the convection heat transfer coefficient on the outer surface of the pipe and inside the pipe in the heat exchanger using the formula formulated by Holman (2010) in Equation 3 and Equation 4.

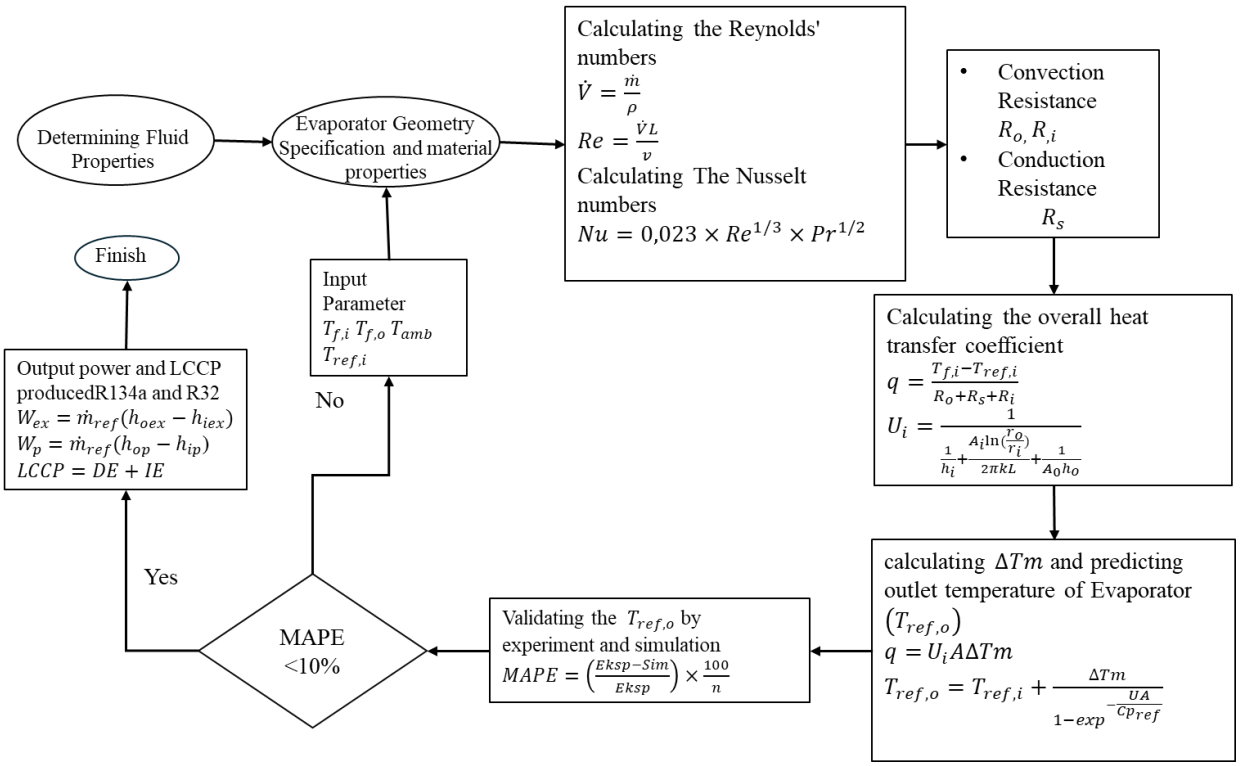

Figure 3. Flow chart of simulation process

$$\boldsymbol{h_o = \frac{Nu \times k_f}{D_o}} \tag{3}$$

$$\boldsymbol{h_i = \frac{Nu \times k_{ref}}{D_i}} \tag{4}$$

where h_o and h_i is respectively outer and internal tube convection coefficient (W/m^2.°C), Nu is Nusselt number, D_o and D_i is outer and inner diameter (m) of the tube, k_f is flue gas thermal conductivity (W/m.°C), and k_{ref} is thermal conductivity of R32 and R134a (W/m.°C).

Before performing calculations on Equations 3 and 4, the type of flow in the evaporator is determined by calculating the Reynolds number, while the Reynolds number is a parameter for determining the Nusselt number, the Reynolds number is calculated using Equation 5 and the Nusselt number is calculated using Equation 6.

$$\boldsymbol{Re = \frac{V \times L}{v}} \tag{5}$$

$$\boldsymbol{Nu = 0.332 Re^{1/3} Pr^{0.5}} \tag{6}$$

where Re is Reynolds number, V is volumetric velocity (m^3/s), v is kinematic viscosity (m^2/s), and L is evaporator length (m).

The total heat transfer coefficient in this study is based on the area inside the copper tube. General equation for calculating the overall heat transfer coefficient (U) was based on Holman (2010) as in Equation 7 and Equation 8.

$$\boldsymbol{q = \frac{T_{f,i} - T_{ref,i}}{\frac{1}{h_o A_o} + \frac{A_i ln(r_o/r_i)}{2\pi k_t L_t} + \frac{1}{h_i A_i}}} \tag{7}$$

$$\boldsymbol{U_i = \frac{1}{\frac{1}{h_i} + \frac{A_i ln(r_o/r_i)}{2\pi k_t L_t} + \frac{A_i}{A_o h_o}\frac{1}{}}} \tag{8}$$

After obtaining some of the results above, a prediction is made of the evaporator outlet temperature which is then applied to the ORC system, by first calculating the average logarithmic temperature difference in the heat transfer process using Equation 9.

$$\boldsymbol{q = U_i \times A \times \Delta T_m} \tag{9}$$

After the value ΔT_m is obtained, a substitution is performed using Equation 10.

$$\boldsymbol{T_{ref,o} = T_{ref,i} + \frac{\Delta T_m}{1 - e^{-\frac{U_i A}{Cp_{ref}}}}} \tag{10}$$

where $T_{f,i}$ is flue gas inlet temperature (℃), $T_{ref,i}$ is R32 and R134a inlet temperature (℃), $T_{ref,o}$ is evaporator outlet temperature of R32 and R134a (℃), U_i overall heat transfer coefficient (W/m.℃), and A is heat transfer area (m).

Table 1Research matrix

$\dot{m}$ fuel (kg/h)	$T_{in,flue\ gas}$ (℃)		Evaporator outlet temperature experiment (℃)				Evaporator outlet temperature simulation (℃)			
	Sengon	Gamal	Sengon (ES)		Gamal (EG)		Sengon (SS)		Gamal (SG)	
			R134a	R32	R134a	R32	R134a	R32	R134a	R32
3.75 (A)	217.8	183.9	P1	P2	P3	P4	S1	S2	S3	S4
2.5 (B)	159.1	158.4	P5	P6	P7	P8	S5	S6	S7	S8

This research matrix is presented in the form of Table 2. To validate the calculations obtained based on the simulation, validation was carried out on the temperature parameters of the R32 and R134a fluids exiting the evaporator outlet using the Mean Absolute Percentage Error (MAPE) in Equation 11. Meanwhile, the evaluation scale can be seen in Table 3.

$$\boldsymbol{MAPE = \left(\frac{eksp - sim}{eksp}\right) \times \frac{100}{n}} \tag{11}$$

Table 2Evaluation scale

Range	Information
<10%	The estimation model is very good
10-20%	Good estimation model
20-50%	Feasible estimation model
>50%	Bad prediction model

2.3. Life Cycle Climate Performance

In this study, CO_2 traces were calculated using LCCP analysis. The LCCP calculation considers direct and indirect emissions. The equation used to calculate LCCP refers to IRR (2016) and (He *et al*., 2024) using Equation 12.

$$\boldsymbol{LCCP = DE + IE} \tag{12}$$

The amount of CO_2 emissions in the LCCP method is presented in the form of $kgCO_2e$, Direct emissions are related to refrigerant leakage and its degradation in the atmosphere, direct emissions are calculated using Equation 13. While indirect emissions are related to annual energy consumption, materials used in the system and emissions from material disposal at the end of life. The general equation used to calculate indirect emissions is Equation 14. The AEC parameter is the annual energy consumption calculated using Equation 15.

$$\boldsymbol{DE = FC \times (LT \times ALR + EOL) \times (GWP + ADP.GWP)/Wnet} \tag{13}$$

$$IE = LT{\times}AEC{\times}EM + \Sigma(m.MM) + \Sigma(mr.RM) + FC{\times}(1 + LT{\times}ALR) \times RFM + FC{\times}(1 - EOL){\times}RFD/Wnet \tag{14}$$

$$\boldsymbol{AEC = Q_h \times O_t} \tag{14}$$

where *DE* is direct emissions ($kgCO_2e$), *IE* is indirect emissions, *FC* is refrigerant mass (kg), *LT* is equipment usage mass (year), *ALR* is annual leakage rate (%), *EOL* is refrigerant loss at end of service life (%), *GWP* is global warming potential, *ADP.GWP* is GWP of the atmospheric degradation product, *AEC* is annual energy consumption (kWh), *RFM* is refrigerant manufacturing emissions, *m* is system mass unit (kg), *mr* is mass of material discharge (kg), *MM* is CO_2 produced by the material, Q_h is heating energy from the evaporator (kJ/s), and O_t is operating hours (h).

The assumptions used to calculate LCCP are based on the International Institute of Refrigeration guidelines (IRR, 2016) presented in the form of Table 4.

Table 4. Input parameters for LCCP calculation

Parameter	R32	R134a	Unit
Mass	1	1	kg
Mass use of equipment	40	40	years
Annual leakage rate (ALR)	4	4	%
EOL	15	15	%
Global Warming Potential	675	1,300	$kgCO_{2e}/kg$
Adp.GWP	N/A	1.6	$kgCO_{2e}/kg$
Emission factor	0.757	0.757	$kgCO_{2e}/kg$
ORC system mass	223.35	223.35	kg
MM	1.43	1.43	$kgCO_{2e}/kg$
mr steell	0.54	0.54	$kgCO_{2e}/kg$
RFM	7.2	5.0	$kgCO_{2e}/kg$
Operating hours	24	24	h
Refrigerant Discharge Emissions (RFD)	N/A	N/A	$kgCO_{2e}/kg$

3. RESULTS AND DISCUSSION

3.1. Evaporator outlet temperature profile

The function of the evaporator is to supply heat by convection and conduction to the working fluid so that the working fluid undergoes a phase change, at least from saturated liquid to saturated vapor. In the observations we made, the evaporator exit temperature when using R32 working fluid with gamal biomass as the energy source reached an average temperature of 86.83℃, while R32 with sengon biomass reached an average temperature of 83.9℃, R134a was 88.49℃. The average temperature of the flue gas in the combustion process of gamal biomass reached 153.04℃, while the average temperature of the flue gas in the combustion process of sengon biomass reached 159.37℃. The difference in flue gas temperature produced in the combustion process is caused by the difference in the calorific value of the biomass used, from the test results with NO. RA/115/08/2023 calorific value of gamal is 4274 Kcal/kg, while the calorific value of sengon is 4281 Kcal. Based on the test results, between gamal and sengon produce temperatures with insignificant differences. Based on this explanation, it can be concluded that the use of gamal and sengon has the same performance in terms of fuel. The temperature profile exiting the evaporator is presented in Figure 4.

3.2. Simulation Validation

Figure 5 shows the results of the evaporator outlet temperature in the experimental and simulation. The figure shows that there is a difference between the simulation and experimental values. The smallest deviation value is 0.32℃ and the largest deviation value is 20.62℃. The largest deviation value is caused by the ash in the furnace being too high, thus inhibiting heat transfer. Meanwhile, Table 5 shows the APE AND MAPE values for all tests. When the temperature deviation value is 0.32℃, the APE value that occurs is 0.55%, while when the temperature deviation value is 20.62℃, the APE value that occurs is 22.31%. Meanwhile, the MAPE value that occurs with a validation number of 8 experiments is 7%. Based on the MAPE standard, this model can be used.

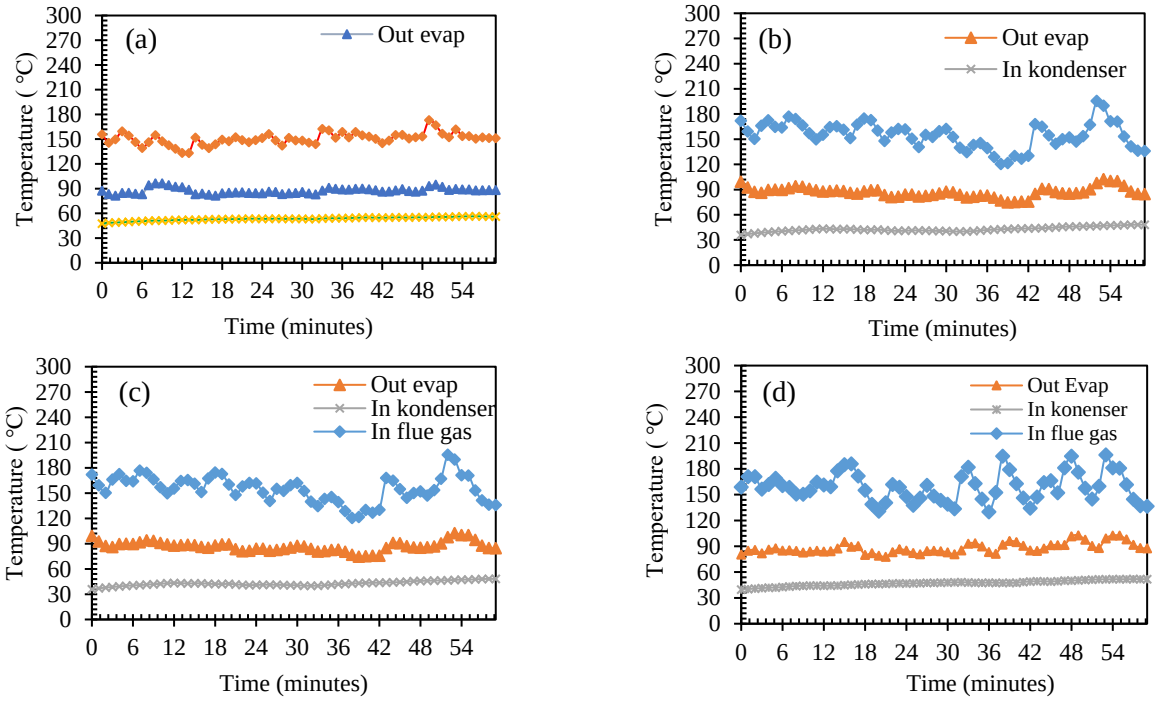

Figure 4. Evaporator outlet temperature profile graph (a) GamalR32 (b) GamalR134a (c) SengonR32 (d) SengonR134a

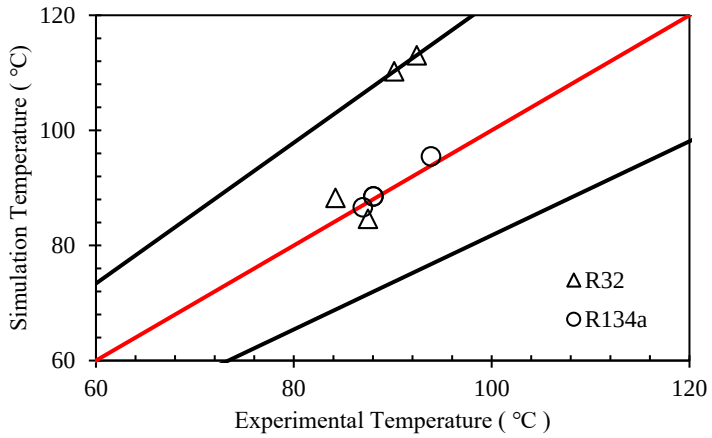

Figure 1Evaporator outlet temperature validation results

Table 5. MAPE Values of the Models Used

Testing Matrix	Evaporator Outlet Temperature (Experiment) (℃)	Evaporator Outlet Temperature (Simulation) (℃)	Delta Experiment and Simulation (℃)	Absolute Percentage Error (APE) (%)	Mean Absolute Percentage Error (%)
P1	86.97	86.65	0.32	0.36	7
P2	92.42	113.05	20.62	22.31	
P3	93.86	95.48	1.62	1.72	
P4	90.15	110.27	20.12	22.32	
P5	87.49	84.63	2.86	3.27	
P6	88.03	88.52	0.48	0.55	
P7	88.03	88.52	0.48	0.55	
P8	84.21	88.27	4.06	4.82	

3.3. Effect of Flue Gas Mass Flow Rate on Evaporator Outlet Temperature

In a shell and tube heat exchanger system, decreasing the flue gas mass flow rate can cause the refrigerant outlet temperature to be lower. The fluid temperature of R134a reaches 142.76℃ at a flue gas mass rate of 0.028 kg/s, when compared to R32 at the same flue gas mass rate, the evaporator outlet temperature reaches 152.47℃. When the flue gas flow rate is reduced by 0.0179 kg/s, it causes the evaporator outlet temperature to decrease linearly. The evaporator outlet temperature when using R32 is 83.02℃ while R134a reaches a temperature of 77℃. This phenomenon can be seen in Figure 3. The phenomenon in Figure 3 explains that the same heating temperature and flow rate result in a higher working fluid temperature of R32 compared to R134a, due to higher evaporation pressure, lower specific heat which means R32 will absorb less heat to increase its temperature, then the latent heat of vaporization of R32 is lower than R134a, as a result the amount of energy required to evaporate R32 is lower than that required by R134a.

Bai *et al*. (2020), have compared 5 working fluids applied to heat pumps, the study reported that the average evaporation pressure of R32 was higher than that of R134a at the same ambient temperature conditions. The low temperature of the working fluid at the evaporator outlet when reducing the mass flow rate of flue gas is influenced by the convection heat transfer coefficient becoming smaller, because the flow becomes more laminar. In addition, the transfer of energy in the form of heat will be reduced, this means that less energy is transferred to the working fluids R134a and R32 so that the outlet temperature is lower. Previous studies have reported the same phenomenon in unidirectional and countercurrent heat exchangers, where decreasing the mass rate can reduce the overall heat transfer coefficient which results in a lower working fluid outlet temperature (Kannojiya *et al*., 2018). The effect of the flue gas mass rate on the evaporator outlet is presented in graphical form in Figure 6.

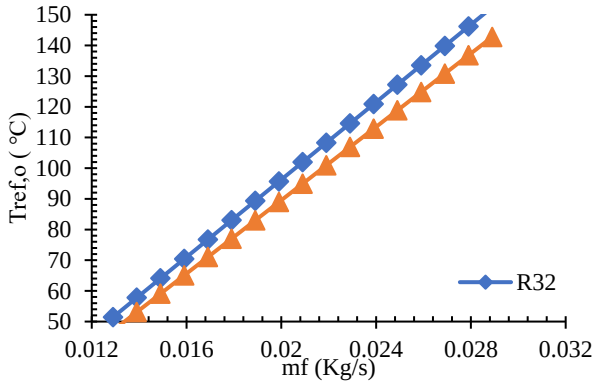

Figure 6. Effect of flue gas mass flow rate on evaporator outlet temperature.

3.4. ORC Performance Based on Flue Gas Rate

In the p-h diagram presented in Figure 4, there are 2 saturation lines, namely liquid and vapor saturation, the left line is the liquid saturation line, while the right is the vapor saturation line. According to Moran *et al*. (2011), in an ideal cycle there are several processes that can be defined, namely the process that passes through the evaporator and pump will be isentropic, meaning there is no irreversibility and heat transfer with the environment. The results of the study in Figure 4 explain the working principle of the ORC cycle ideally starting from the working fluid entering the pump at condition 4-1 as a saturated liquid and compressed to the operating pressure to the evaporator at condition 1-2. The temperature of the working fluid will increase during isentropic compression because its specific volume decreases. The working fluid enters the evaporator at condition 2-3 as a compressed liquid and will become superheated vapor. The superheated vapor then enters the expander at condition 3-4 to be expanded by the expander which then produces work to rotate the shaft. Pressure and temperature will decrease during this process to condition 4 where the steam will enter the condenser, the steam will be changed into liquid phase at constant pressure in the condenser and will enter the pump as saturated liquid (Cengel & Boles, 2015). This research is presented in Figure 7.

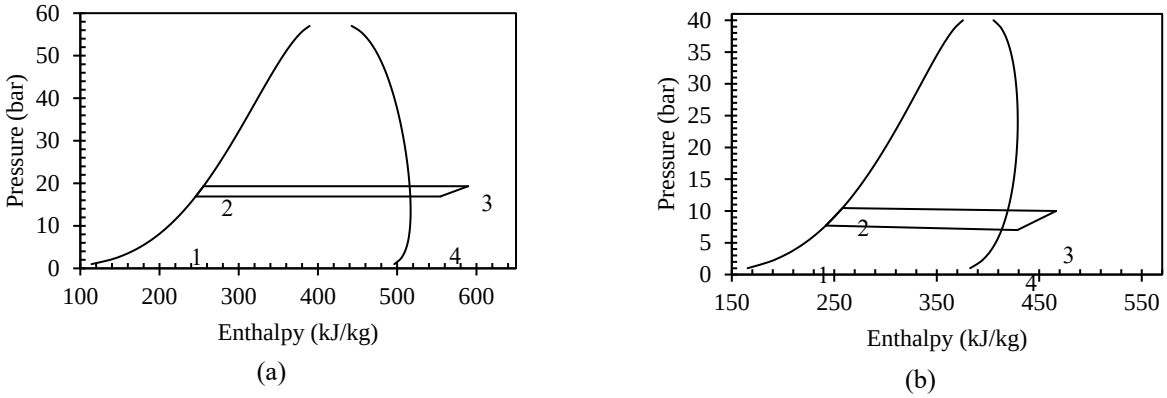

Figure 7. Pressure and enthalpy diagram (a) working fluid R32 (b) working fluid R134a

Pressure measurement in this study was only carried out at the evaporator outlet, to estimate the power generated in the system, a simulation was first carried out using REFPROP to determine the enthalpy of each working fluid by configuring the quality of the pump inlet at liquid saturation. At a working fluid mass flow rate of 0.0054 kg/s, R134a is able to produce a turbine output power of 0.206 kW with a pump working power of 0.08 kW so that the net power generated in the ORC system that we observed reached 0.126 kW at an evaporator outlet pressure of 10 bar. While R32 output power generated is 0.18 kW with a pump working power of 0.05 kW, so that the net power generated in the ORC system using the R32 working fluid reaches 0.14 kW at a pressure of 19 bar. As stated in Figure 2, pressure and temperature are measured in the ORC at each component (inlet and outlet). Temperature and pressure are required as input to obtain the properties of the working fluid. Flue gas from the combustion furnace is used to evaporate the working fluid in the evaporator. The evaporator temperature and flow rate of both flue gas and working fluid affect heat transfer. The relationship between temperature and flow rate in flue gas and working fluid is linear, the higher the temperature and flow rate in flue gas with a constant working fluid flow rate will produce a higher temperature.

The type of working fluid and the evaporator outlet temperature play an important role in increasing the efficiency of the ORC system. The temperature difference in this study is not much different because the energy carried by the flue gas is relatively small. At a fuel mass rate of 2.5 kg/s, the flue gas energy entering the evaporator reaches 0.90 kJ/s while at a fuel mass flow rate of 3.75 kg/s the flue gas energy entering the evaporator reaches 0.95 kJ/s, the energy difference which is not much different in this study is also caused by the air flow rate supplied to the constant biomass combustion process. Previous studies have reported that the thermal efficiency of the R32 working fluid has better performance compared to R134a (Hartulistiyoso *et al*., 2020). In addition, an in-depth analysis of the working fluid applied to the ORC system is needed, because working fluids with a cyclic structure provide higher efficiency (Zhai *et al*., 2014). The output power in our study is relatively lower than those of Hartulistiyoso *et al*. (2020), that can be caused by the relatively lower mass flow rate of the working fluid we used. By reducing the mass flow rate of the working fluid, it causes the residence time of the working fluid in the evaporator to be longer. This means that the working fluid has a longer time to interact with the heat transfer surface to achieve thermal equilibrium with the flue gas or with the heat exchanger wall, resulting in a higher evaporator outlet temperature. Muslim *et al*. (2019), reported that the optimum operating temperature of R134a was 100°C with a mass rate of 0.036 kg/s capable of producing output power of up to 3.22 kW. In addition, to increase the output power in the ORC system by increasing the working mass rate of the working fluid (Upadhyaya & Gumtapure, 2018). The output power of our study is showed in Table 6.

Table 6. ORC output power

Fuel rate (kg/s)	Working Fluid	Evaporator Outlet Temperature (°C)	Power (kW)
2.5	R134a	83.91	0.12
	R32	86.83	0.14
3.75	R134a	90.1	0.15
	R32	91.29	0.16

3.5. Life Cycle Climate Performance

In this paper testing, emission analysis is focused on the ORC system. The source of flue gas used as a heat source comes from a furnace with biomass fuel. As we all know, biomass has characteristics as Carbon Neutral. The concept of "Carbon Neutral" or carbon neutral in the context of biomass refers to a condition where the amount of carbon dioxide (CO_2) released into the atmosphere from biomass combustion is equal to the amount of CO_2 absorbed by plants as they grow. In other words, the use of biomass does not increase the total amount of CO_2 in the atmosphere net (Green & Byrne, 2004). In addition, the concept of calculating emissions in this paper is focused on ORC using the LCCP method. LCCP focuses on the use of refrigerant as a working fluid, based on the explanation above so that the fuel emission value is not included in the emission calculation.

As mentioned above, LCCP is a calculation method for analyzing carbon footprints directly and indirectly (IRR, 2016). In this study, the LCCP value of each working fluid used is presented in Figure 8. Working fluids with higher GWP values have the potential to increase direct emissions higher than working fluids with lower GWP, as can be seen in figure, R32 with a GWP of 675 $kgCO_2e/kg$ contributes direct emissions of up to 1,181 $kgCO_2e/kg$ when compared to the working fluid R134a, the direct emissions (DI) produced reach 2,277 $kgCO_2e/kg$. Kim *et al.* (2020), have observed the same phenomenon by comparing R32 with R410A, the study stated that R32 has the potential to increase direct emissions much lower than R410A. The emission value directly impacts the LCCP value produced by each fluid, the LCCP value produced by R32 reaches 2,546 $kgCO_2e$ while R134a reaches 3,592 $kgCO_2e$, if converted per unit of output power, the emission of R32 reaches 13,774 $kgCO_2e/kW$ while R134a is 17,420 $kgCO_2e/kW$. Basically, the LCCP method results in an absolute value in $kgCO_2e$ units if referring to the latest International Institute of Refrigerant (IRR) paper on LCCP calculations by He *et al.* (2024), the LCCP value is compared with the power required in $kgCO_2e/kW$ units in the refrigeration system. The results of the LCCP calculation are presented in Figure 8.

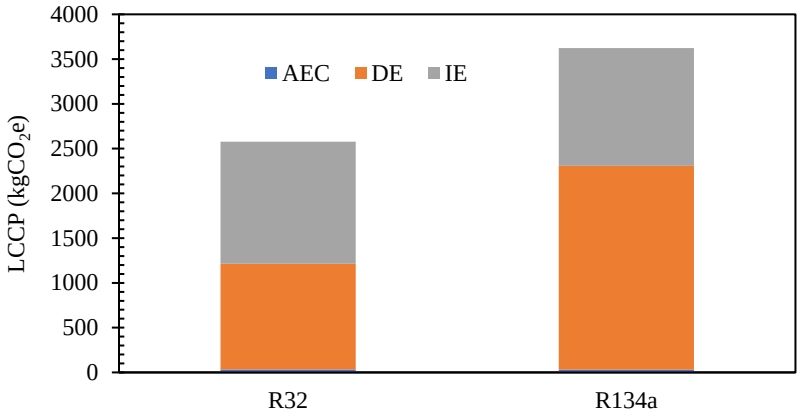

Figure 8. LCCP calculation results.

4. CONCLUSION

The simulation results in this study show a very good MAPE value because <10%. The decrease in flue gas temperature can cause the temperature of the working fluid R134a and R32 coming out of the evaporator to be lower due to the convection heat transfer coefficient becoming smaller and the transfer of energy in the form of heat is reduced. While the output power of R134a produced is smaller than R32. The value of the CO_2 contribution produced based on the LCCP calculation for R32 is lower than R134a.

ACKNOWLEDGEMENTS

The author would like to thank the Osaka Foundation through PPLH IPB University 2023 with project number PPJ-261200-232452 which has funded this research to evaluate the specific energy in sawdust production by comparing 4 and 2 production steps and continued with the use of sawdust in pellet production and its utilization as energy fuel in

the Organic Rankine Cycle (ORC). We would also like to thank the Indonesian Education Fund Management Institute (LPDP RI) which has provided funds and supported the first author's education at IPB University.

REFERENCES

Alao, M.A., Popoola, O.M., & Ayodele, T.R. (2022). Waste-to-energy nexus: An overview of technologies and implementation for sustainable development. *Clean Energy Systems*, ***3***, 100034. https://doi.org/10.1016/j.cles.2022.100034

Amirta, R., Yuliansyah, Y., Angi, E.M., Ananto, B.R., Setyono, B., Haqiqi, M.T., Septiana, H.A., Lodong, M., & Oktavianto, R.N. (2016). Plant diversity and energy potency of community forest in East Kalimantan, Indonesia: Searching for fast growing wood species for energy production. *Nusantara Bioscience*, ***8***(1), 22–31. https://doi.org/10.13057/nusbiosci/n080106

Ashwni, Sherwani, A.F., & Tiwari, D. (2021). Exergy, economic and environmental analysis of organic Rankine cycle based vapor compression refrigeration system. *International Journal of Refrigeration*, ***126***, 259–271. https://doi.org/10.1016/j.ijrefrig.2021.02.005

Bahrami, M., Pourfayaz, F., & Kasaeian, A. (2022). Low global warming potential (GWP) working fluids (WFs) for Organic Rankine Cycle (ORC) applications. *Energy Reports*, ***8***, 2976–2988. https://doi.org/10.1016/j.egyr.2022.01.222

Bai, C., Han, Z., Wei, H., Ju, X., Meng, X., & Fu, Q. (2020). Simulation study on performance of a dual-source hybrid heat pump unit with alternative refrigerants. *Energy and Built Environment*, ***1***(1), 1–10. https://doi.org/10.1016/j.enbenv.2019.08.004

Çengel, Y.A., & Boles, M.A. (2015). *Thermodynamics: An Engineering Approach* (8th ed.). McGraw-Hill Education.

Dai, X., Shi, L., & Qian, W. (2019). Review of the working fluid thermal stability for organic Rankine cycles. *Journal of Thermal Science*, ***28***(4), 597–607. https://doi.org/10.1007/s11630-019-1119-3

Green, C., & Byrne, K.A. (2004). Biomass: Impact on carbon cycle and greenhouse gas emissions. *Encyclopedia of Energy*, ***1***, 223–236. https://doi.org/10.1016/B0-12-176480-X/00418-6

Hartulistiyoso, E., Sucahyo, L., Yulianto, M., & Sipahutar, M. (2020). Thermal efficiency analysis of Organic Rankine Cycle (ORC) system from low-grade heat resources using various working fluids based on simulation. *IOP Conference Series: Earth and Environmental Science*, ***542***(1). https://doi.org/10.1088/1755-1315/542/1/012047

He, Y., Zheng, Y., Zhao, J., Chen, Q., & Zhang, L. (2024). Study of a novel hybrid refrigeration system, with natural refrigerants and ultra-low carbon emissions, for air conditioning. *Energies*, ***17***(4). https://doi.org/10.3390/en17040880

Hijriawan, M., Pambudi, N.A., Wijayanto, D.S., Biddinika, M.K., & Saw, L.H. (2022). Experimental analysis of R134a working fluid on Organic Rankine Cycle (ORC) systems with scroll-expander. *Engineering Science and Technology, an International Journal*, ***29***, 101036. https://doi.org/10.1016/j.jestch.2021.06.016

Holman, J.P. (2010). *Heat Transfer* (10th ed.). McGraw-Hill Companies, Inc.

International Institute of Refrigeration [IRR]. (2016). *Guideline for Life Cycle Climate Performance* (Version 1.2). International Institute of Refrigerant. https://www.iifiir.org

Kannojiya, V., Gaur, R., Yadav, P., & Sharma, R. (2018). Performance investigation of a double pipe heat exchanger under different flow configuration by using experimental and computational technique. *Archives of Mechanical Engineering*, ***65***(1), 27–41. https://doi.org/10.24425/119408

Kementerian ESDM. (2023). *Capaian Kinerja Sektor ESDM Tahun 2022*.

Kim, B., Lee, D.C., Lee, S.H., & Kim, Y. (2020). Performance assessment of optimized heat pump water heaters using low-GWP refrigerants for high- and low-temperature applications. *Applied Thermal Engineering*, ***181***, 115954. https://doi.org/10.1016/j.applthermaleng.2020.115954

Macchi, E., & Astolfi, M. (2017). *Organic Rankine Cycle (ORC) Power System: Technologies and Applications*. Woodhead Publishing.

Moran, M.J., Shapiro, H.N., Boettner, D.D., & Bailey, M.B. (2011). *Fundamentals of Engineering Thermodynamics* (7th ed.). John Wiley & Sons, Inc.

Muslim, M., Alhamid, M.I., Nasruddin, Yulianto, M., & Marzuki, E. (2019). Cycle tempo power simulation of the variations in heat source. *International Journal of Technology*, ***10***(5), 979–987. https://doi.org/10.14716/ijtech.v10i5.3067

Ono, R., Fukuda, Y., Fujii, M., & Yamagata, Y. (2023). Assessment of unutilized woody biomass energy and the cost and greenhouse gas emissions of woody biomass power plants in Hokkaido, Japan. *Clean Energy Systems*, ***6***, 100084. https://doi.org/10.1016/j.cles.2023.100084

Sucahyo, L., Yulianto, M., Hartulistiyoso, E., & Faza, I. (2020). Thermal efficiency simulation of working fluids performance on small scale organic Rankine cycle (ORC) with biomass energy. *IOP Conference Series: Earth and Environmental Science*, ***542***, 012039. https://doi.org/10.1088/1755-1315/542/1/012039

Thangavel, S., Verma, V., Tarodiya, R., & Kaliyaperumal, P. (2021). Comparative analysis and evaluation of different working fluids for the organic Rankine cycle performance. *Materials Today: Proceedings*, ***47***, 2580–2584. https://doi.org/10.1016/j.matpr.2021.05.064

Upadhyaya, S., & Gumtapure, V. (2018). Thermodynamic analysis of organic Rankine cycle with hydrofluoroethers as working fluids. *IOP Conference Series: Materials Science and Engineering*, ***376***(1). https://doi.org/10.1088/1757-899X/376/1/012026

Yulianto, M., Gupta, C., Hartulistiyoso, E., Nelwan, L.O., & Agustina, S.E. (2022). Thermal characteristics of coconut shells as boiler fuel. *International Journal of Renewable Energy Development*, ***12***(2), 227–234. https://doi.org/10.14710/ijred.2023.48349

Zhai, H., Shi, L., & An, Q. (2014). Influence of working fluid properties on system performance and screen evaluation indicators for geothermal ORC (organic Rankine cycle) system. *Energy*, ***74***, 2–11. https://doi.org/10.1016/j.energy.2013.12.030

Zhang, H.H., Li, M.J., Feng, Y.Q., Xi, H., & Hung, T.C. (2021). Assessment and working fluid comparison of steam Rankine cycle - Organic Rankine cycle combined system for severe cold territories. *Case Studies in Thermal Engineering*, ***28***, 101601. https://doi.org/10.1016/j.csite.2021.101601

Zhao, Y., Wang, S., Ge, M., Li, Y., & Yang, Y. (2018). Energy and exergy analysis of thermoelectric generator system with humidified flue gas. *Energy Conversion and Management*, ***156***, 140–149. https://doi.org/10.1016/j.enconman.2017.10.094